Non- enzymatic detection of 17β-Estradiol in real samples using PANI@CeO_2 nanocomposite

Aditya Dam, Tanu Rajput, Sakshi Verma, D Kumar*

Department of Applied Chemistry, Delhi Technological University, Delhi-110042, India

Abstract

Herein, we introduced a non-enzymatic biosensing platform using polyaniline (PANI) as conducting polymer (CP) matrix grafted with CeO_2. The one-pot synthesized nanocomposite has been used for the sensitive detection of 17β-Estradiol (E2). The homogeneous distribution of CeO_2 onto PANI matrix leads to an increase in surface area and the conductivity of synthesized nanocomposite PANI@CeO_2. The PANI@CeO_2 nanocomposite was characterized using structural and morphological techniques. Further, the electrode fabrication was performed by electrophoretically depositing of PANI@CeO_2 nanocomposite onto ITO. The PANI@CeO_2/ITO showed enhanced electrochemical behaviour as compared to PANI/ITO. Detection of E2 was carried out using differential pulse voltammetry (DPV). Linearity has been observed in the detection range 1 - 100 µM with LOD = 2.15 µM. The developed biosensor has been found to be stable and selective towards E2 and has been successfully utilized for the detection of E2 in real samples such as tap water and human urine sample, encouraging its use for further application in clinical diagnosis and biomedical sciences.

Keywords: Polyaniline, 17β-estradiol, biosensor, tap water, urine, CeO_2

*Corresponding author
Email: dkumar@dce.ac.in
ORCID No. orcid.org/0000-0001-9118-2070

1. INTRODUCTION

The most potent estrogen found naturally is E2. E2 is the female sex hormone produced in ovaries that aid growth and also increase milk yield in cows. Apart from the ovaries, a small amount of this hormone is also produced in the adrenal cortex and the testes. This reason has made its use in animal husbandry skyrocket in recent years [1]. The Water Framework Directive of the European Union has reported the presence of E2 in water samples. E2 may enter the environment from a variety of sources, most commonly through animal and human urine [2]. Toxicological studies have concluded that even if a small amount of E2 residue enters an organism's body via the food chain, it can disrupt the working of the endocrine system, resulting in medical issues like male infertility, damage to the blood-brain barrier, increased chances of obesity, may cause breast and testicular cancer [3,4]. Therefore, to control public and environmental health, a convenient and rapid analytical method for the detection of E2 with high sensitivity is required. Some of the analytical methods used to detect E2 include high-performance liquid chromatography and gas chromatography-mass spectrometer. However, the introduction of biosensors for monitoring and managing E2 have shown drastic sensitive, selective and efficient results in monitoring E2 over the last decade [5]. One most promising method for the detection of this hormone could be using a substrate that can be flexible along with a potent sensing material based on polymers. Polymers with good conducting capabilities like PANI as well as polypyrrole have received a lot of attention in the development of biosensors as they have advantages such as high electrical conductivity, easy preparation, rapid response as well as cost-effectiveness [6,7]. In this concern, enzyme immobilization has gained popularity but this comes with various limitations like high cost, thermal and chemical instability, low sensitivity due to leakage of enzyme from the transducer surface [8,9].

In recent years, Polyaniline (PANI) has been extensively studied as an excellent sensing material because it has high sensitivities, is highly reliable and has low-cost [10]. However, pure PANI materials have some limitations:

- Their long-term stability is poor
- Their response and recovery time is also long

As a result, PANI-based nanocomposite materials, primarily PANI-carbon series nanomaterials have been proposed to improve the performance of flexible PANI-based biosensors [[11]. Nanocomposites which have organic polymers and inorganic metal oxide nanoparticles in nano-scale regimes give rise to a new class of materials with unique properties. It has been reported that nano-structured composites of CP with inorganic nanoparticles exhibit synergetic effects in terms of electrical and mechanical properties. The inclusion of semiconductor metal oxide nanoparticles into polymer matrices has been shown to improve the mechanical, thermal, dielectric, and optical properties of polymers, enabling high carrier mobilities [12,**Error! Reference source not found.**.. In this regard, Cerium oxide (CeO_2) nanoparticles have several advantages for the development of biosensors, including electrocatalytic behaviour, oxygen storage capacity, and optical transparency [[14]. After considering the characteristics of PANI@CeO_2 nanocomposite, the contribution of this work can be summarised as below:

a) This research work reveals fabrication of electrode using synthesized PANI@CeO_2 nanocomposite which acts as an effective sensing platform for E2 detection. PANI matrix grafted with CeO_2 increases the surface area, electrical conductivity and sensitivity of nanocomposite.

b) The performance of PANI@CeO_2 composite as a sensing platform has been analyzed in real samples, i.e., human urine and tap water.

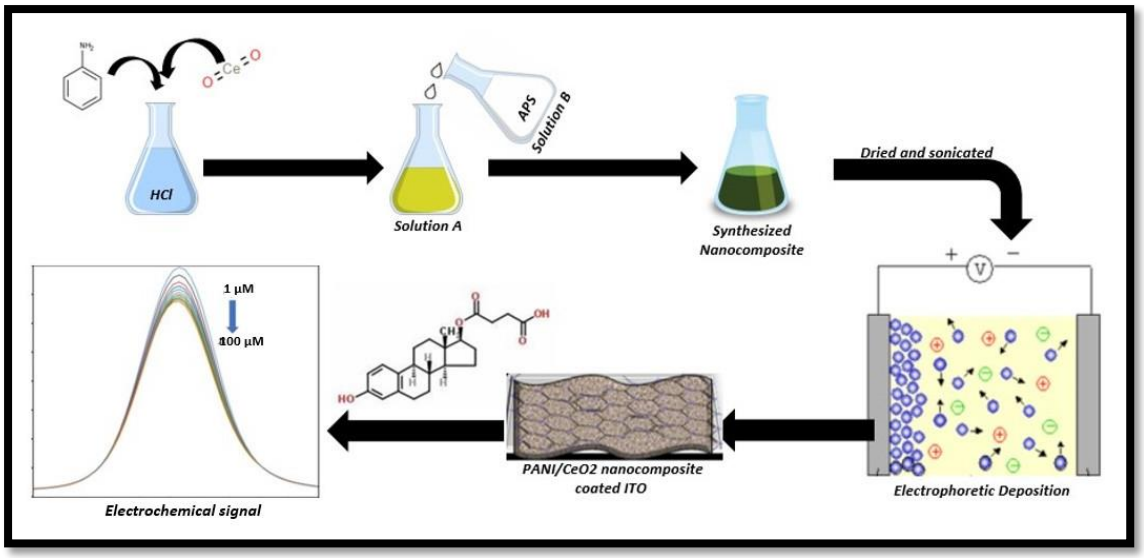

Fig. 1 Schematic diagram of deposition of PANI@CeO_2 biosensing platform for E2 detection

2. MATERIALS AND METHODS

2.1. Materials required

Aniline and ammonium persulfate, bought from Central Drug House (Pvt). Cerium (III) nitrate hexahydrate (Ce $(NO_3)_3 \cdot 6H_2O$, 99%) was procured from Sigma Aldrich. Hydrochloric acid (HCl, 25-26%) and liquor ammonia (25%) procured from Thermofischer Scientific, India. Di-sodium hydrogen orthophosphate dihydrate, sodium dihydrogen orthophosphate, potassium ferrocyanide, potassium ferricyanide were purchased from Qualigens Fine Chemicals. The cleaning was done using 100% acetone and 99.9% ethanol.

2.2. Synthesis of PANI

For the synthesis of PANI, we took 1 mL of aniline and added it to 15 mL HCl (1 M) to get solution-A. Then, solution-B was prepared by dissolving ammonium persulphate in 15 mL HCl (1M). The molar ratio of aniline and ammonium persulphate was taken to be 1:1.15 respectively. At 0-5°C, solution-B was added drop-wise into solution-A followed by 3 h of stirring under the same condition. At last, the resultant solution was kept overnight in the refrigerator and rinsed with acetone and distilled water next day to remove impurities. The

product so obtained was then filtered, dried in an oven at 60°C to get dark green coloured PANI [[15].

2.3. Synthesis of CeO_2

For the synthesis of CeO_2 nanoparticles, $Ce(NO_3)_3 \cdot 6H_2O$ (1.5 mmol) was dissolved in distilled water (50 mL) followed by the addition of 1.5 mL of liquor ammonia. The solution was then stirred for 30 min using a magnetic stirrer. Following this, the solution mixture was transferred to an autoclave (120 mL) and heated up to 180°C for 24 h in an oven. Obtained stagnant was then cooled at room temperature, washed several times with ethanol and distilled water for the excretion of excessive ammonium hydroxide and was dried at 60°C for 24 h to get the desired pale-yellow white coloured product.

2.4. Synthesis of PANI@CeO_2 nanocomposite

For synthesis of PANI@CeO_2 nanocomposite, 40 % (w/w) of synthesized CeO_2 was added to 1 mL of aniline in 15 mL HCl (1 M) to get solution-A followed by the same procedure as mentioned in the synthesis of PANI.

2.5. Electrophoretic deposition (EPD) on electrode

We deposited all three synthesized compounds (0.1 mg/mL) electrophoretically on ITO (Indium Tin oxide) coated glass electrode taking platinum as the counter electrode. The EPD process was conducted at a constant voltage of 10 V provided via a DC power supply for stable deposition for 7 sec in case of PANI and CeO_2 suspension and for PANI@CeO_2 nanocomposite suspension it was optimized at 15 sec. After EPD, the electrodes were removed from the suspension and stored in a refrigerator for further use.

2.6. Characterization

For structural characterization, we used Cu Kα radiations (λ= 1.5406 Å) based Bruker D-8 Advance X-ray diffractometer (XRD), Perkin-Elmer Fourier transforms infrared (FT-IR) spectrum (Model Spectrum 2), TGA 4000, Perkin Elmer range 0-600° C in N_2 atmosphere with a constant heating rate of 10° C/min. For electrochemical studies, we used Autolab potentiostat/galvanostat (Eco-Chemie, the Netherlands), comprising three-electrode cell consisting of platinum and Ag/AgCl as inert and auxiliary electrode in phosphate buffer saline (PBS; pH 7.4; 100 mM) containing ferrocyanide and ferricyanide $[Fe(CN)_6]^{3-/4-}$ of 5 mM concentration each.

3. RESULTS AND DISCUSSION

3.1. XRD

The powder XRD pattern of CeO_2, PANI@CeO_2 nanocomposite and PANI has been shown in the **Fig. 2A** and **Fig. S1**. It has been observed that CeO_2 shows clearly distinct XRD peaks at 2θ = 28.5°, 33.1°, 47.7°, 57.1°, 59.3°, 69.6°, 77.0° and 79.2° which correspond to the (111), (200), (220), (311), (222), (400), (331) and (420) Bragg's crystal plane reflections, respectively [[17]. The observed diffraction peaks of the synthesized CeO_2 satisfied the fluorite-type crystal cubic phase of CeO_2 (JC-PDS card no 01-075-8371) [[16].

In the XRD pattern of PANI@CeO_2 nanocomposite, it has been observed that the diffraction peaks of PANI and CeO_2 overlapped with each other. Both the PANI and PANI@CeO_2 nanocomposite show a broad peak located at 2θ = 26° satisfying the amorphous of PANI. The synthesized PANI@CeO_2 nanocomposite shows rest of the peaks parallel to peaks of CeO_2 indicating its successful synthesis.

3.2. FT-IR

The FT-IR spectra CeO_2, PANI@CeO_2 nanocomposite and PANI has shown in the **Fig. 2B** and **Fig. S2**. For PANI@CeO_2 nanocomposite a small sharp peak at 1299 cm^{-1} is due to the C-N stretching of secondary aromatic amine. The wide and sharp peak at 1130 cm^{-1} corresponds to the bending vibration of C-H. The very small and clear peaks at 803 cm^{-1} indicate the metal-oxygen bands. The small peak at 1244 cm^{-1} shows the C-N and C-C stretching bands of PANI. The sharp peak at 1487 cm^{-1} shows the benzenoid ring stretching of PANI. The wide peak at 503 cm^{-1} corresponds to the metal-oxygen stretching frequency whose intensity increases with increase in content of CeO_2 in the PANI@CeO_2. For pure CeO_2 this peak was observed at 496 cm^{-1} and shifted to 503 cm^{-1} in case of PANI@CeO_2 which illustrates the weak interaction between CeO_2 and PANI, while other prominent peaks of pure CeO_2 are 619, 1126, 1356 and 1569 cm^{-1} which attribute to the stretching band of metal-oxygen bond [18,[19].

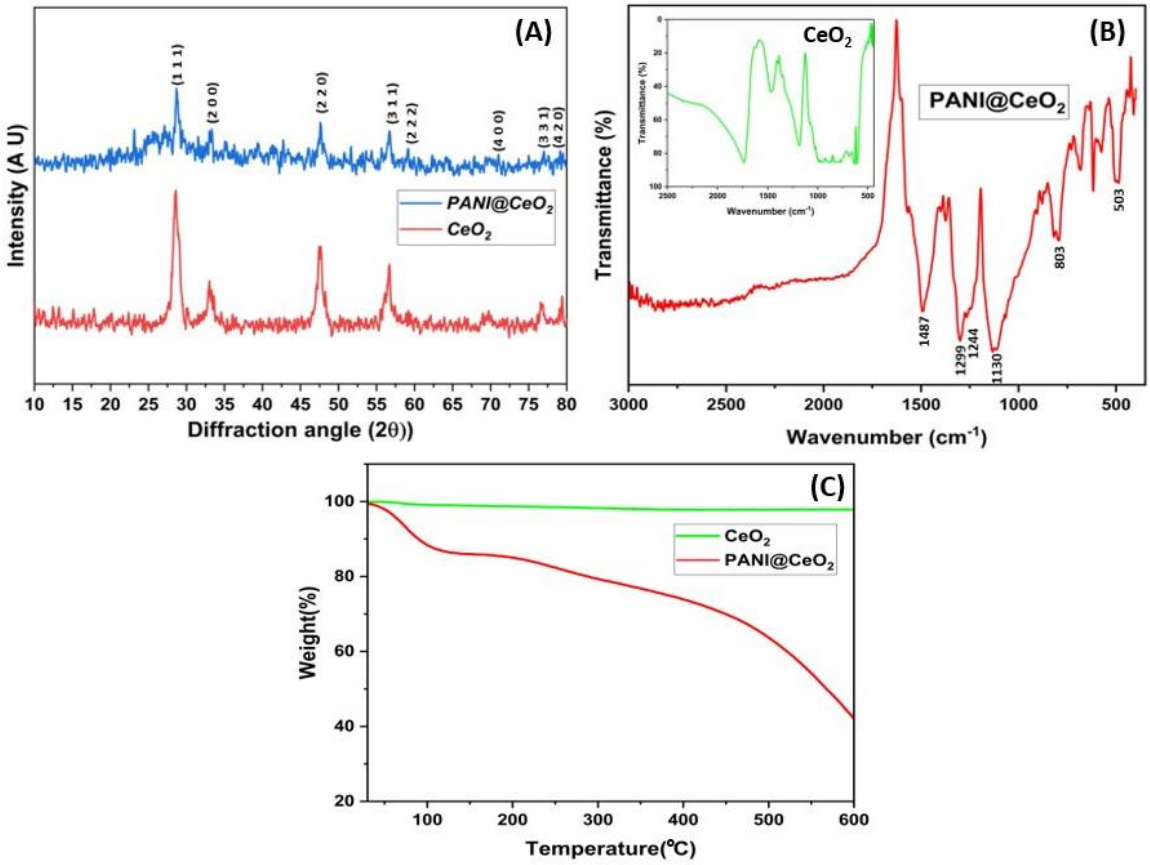

Fig. 2 A) XRD spectra; B) FT-IR spectra and C) TGA plot of PANI@CeO_2 and CeO_2

3.3. Thermogravimetric analysis

From the TGA thermogram of CeO_2 an PANI/CeO_2 as shown in **Fig. 2C**, it is observed that pure CeO_2 crystals are superiorly stable and thermally resistant in the temperature range of 20-600 °C whereas PANI@CeO_2 nanocomposite shows loss in its mass in two steps. The first decrease in mass of about 10% occurs in the range of 40-100 °C due to the loss of water from PANI chains. In the second step loss of mass occurs in the range of 250-600 °C corresponding to the decomposition of polymeric chains. The more the content of CeO_2 in the composite, the more strengthening occurs between the polymeric chains and CeO_2 and the thermal decomposition of the chains is restricted accordingly [20,[20].

3.4. Morphological studies

The surface morphology of PANI and PANI@CeO_2 was analysed using scanning electron microscope (SEM) which are shown in **Fig. 3A** and **3B** respectively. The morphology of PANI is observed to be grain like structure which contains some pores and voids. From the morphology of PANI@CeO_2 nanocomposites, it was observed that PANI@CeO_2 have some spherical and irregular shaped grains with diameter in nano range, where the CeO_2 nanoparticles are homogeneously compacted in the PANI matrix leading to homogeneous morphology and the higher conductivity of PANI@CeO_2 nanocomposite.

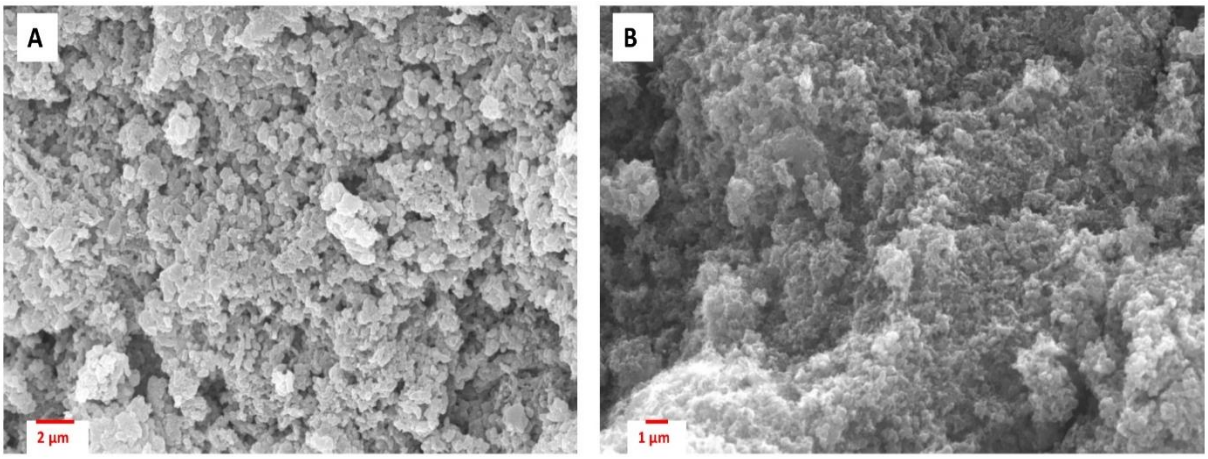

Fig. 3 SEM images of A) PANI and B) PANI@CeO_2 nanocomposite

4. ELECTROCHEMICAL STUDIES

4.1. Electrochemical studies of electrodes

Electrochemical studies of the PANI/ITO and PANI@CeO_2/ITO electrodes have been performed using cyclic voltammetry (CV) technique in PBS (pH-7.4; 100 mM) containing $[Fe(CN)_6]^{3-/4-}$. At 50 mV/s, it was observed that PANI@CeO_2 electrode exhibits higher current as compared to the PANI/ITO electrode, which illustrates the better electron conduction ability of the PANI@CeO_2/ITO electrode. **Fig. 4A**.

Scan rate study has also been performed for both the electrodes as shown in **Fig. 4B and Fig. S3**. It is observed that the anodic peak potential increases from 10 mV/s to 300 mV/s and the cathodic peak potential decreases with increase in the scan rate for both the PANI and PANI@CeO_2/ITO electrodes. This led to a linear relation between the anodic and cathodic peak potentials (E_{pa} and E_{pc}) of PANI and PANI@CeO_2 with respect to logarithmic scan rate (log ν) **[Fig. 4D]**[equations 1 to 4] [22]. A linear correlation between the anodic and cathodic peak current (I_{pa} and I_{pc}) with respect to square root of scan rates ($\nu^{1/2}$) has also been observed from the scan rate studies of PANI and PANI@CeO_2/ITO electrodes **[Fig. 4C]** and has been depicted by equations 5 to 8.

E_{pa} [PANI@CeO_2/ITO] = 0.04968V log (ν) + 0.148V; R^2 = 0.9492 (1)

E_{pc} [PANI@CeO_2/ITO] = −0.0708V log (ν) + 0.183V; R^2 = 0.9710 (2)

E_{pa} [PANI/ITO] = 0.1075V log (ν) + 0.1187V; R^2 = 0.9833 (3)

E_{pc} [PANI/ITO] = −0.2257V log (ν) + 0.3403V; R^2 = 0.8701 (4)

I_{pa} [PANI@CeO_2/ITO] = 2.75×10^{-5} A/mV/s x $\nu^{1/2}$ + 4.483×10^{-5} A; R^2 = 0.994 (5)

I_{pc} [PANI@CeO_2/ITO] = -1.77×10^{-5} A/mV/s x $\nu^{1/2}$ – 7.008×10^{-5}A; R^2 = 0.978 (6)

I_{pa} [PANI/ITO] = 1.66×10^{-5} A/mV/s $\nu^{1/2}$ + 5.6315×10^{-5} A; R^2 = 0.9905 (7)

I_{pc} [PANI/ITO] = -9.31×10^{-6} A/mV/s x $\nu^{1/2}$ – 6.422×10^{-5} A; R^2 = 0.9855 (8)

Using above linear equations and equations S1 to S4, the value of electron transfer co-efficient (α), charge transfer rate constant (K_s), average surface coverage (λ), diffusion co-efficient for $[Fe(CN)_6]^{3-/4-}$ solution (D) and effective surface area of electrodes (A) were calculated for both PANI and PANI@CeO_2/ITO electrodes and has been summarized in Table 1. The values of D and A are greater for PANI@CeO_2 nanocomposite than PANI, because PANI@CeO_2

performs better diffusion of redox ions through its active detection area and electrode interface [23,24].

Table 1

Electrodes	Electron transfer co-efficient (α)	Charge transfer rate constant (K_s)(s^{-1})	Average surface coverage (λ)(m^{-2})	Diffusion co-efficient (D)(m^2s^{-1})	Effective surface area (A)(m^2)
PANI/ITO	0.9138	0.1804	$1.515x10^{-4}$	$4.964x10^{-4}$	$5.22x10^{-7}$
PANI@CeO_2/ITO	0.8874	0.8184	$2.07x10^{-4}$	$9.5x10^{-4}$	$6.32x10^{-7}$

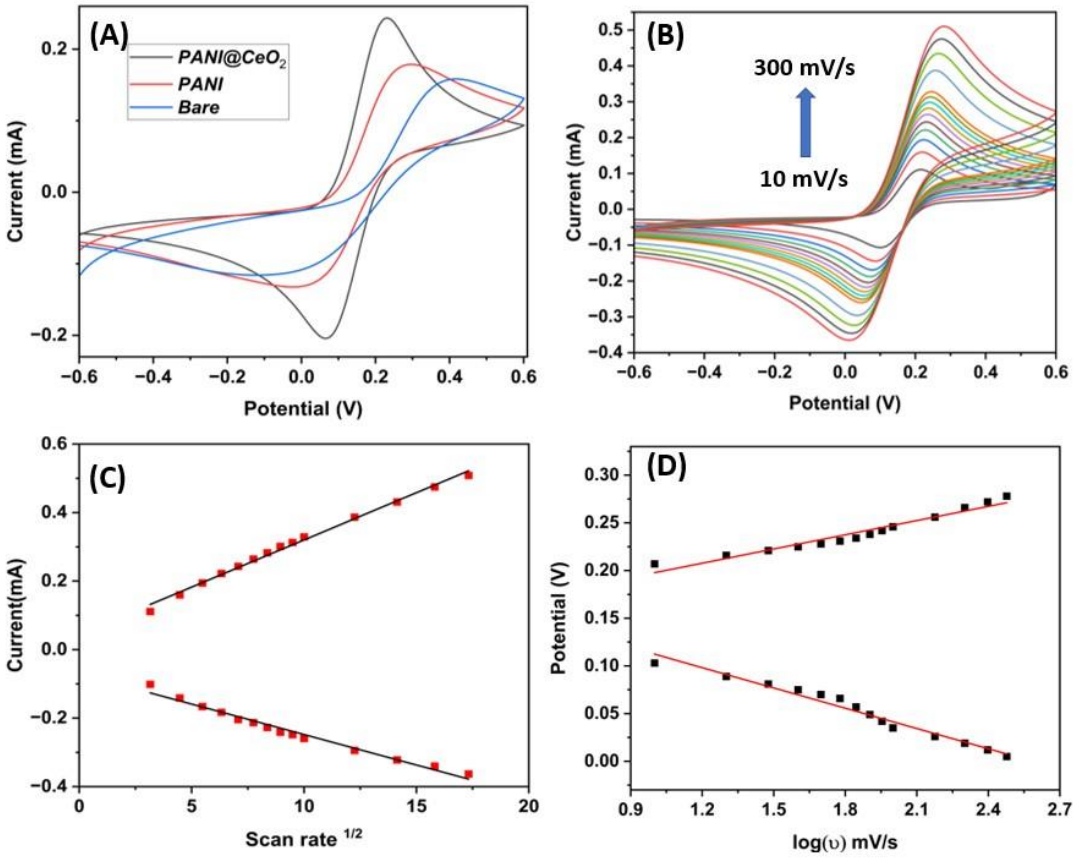

Fig. 4 A) CV studies of PANI@CeO_2, PANI and CeO_2; B) Scan rates study of PANI@CeO_2 electrode (10-300 mV/s); C) Plot of I_{pa}, I_{pc} vs. $v^{1/2}$ and D) Plot of potential vs. log ν for PANI@CeO_2 electrode

4.2. Optimization of pH parameter

To increase the sensing efficiency of the electrodes, it is necessary to optimize the pH value of the electrolyte solution as the pH affects the sensitivity of the electrode towards analyte. Thus, we performed the optimization of buffer solution from pH-5.5 to pH-8.5 using the DPV. Maximum current has been observed at pH-7.4 and thus we used pH 7.4 buffer for all the sensing studies **(Fig. S4**). This can be attributed to the fact that as the rate of deprotonation of phenols decline with rise in pH of the solution. Also, human body serum has an optimum pH 7.4, hence this pH is favourable for clinical studies as well.

4.3. Electrochemical biosensing of 17β-estradiol

The electrochemical sensing of E2 was performed using DPV technique in optimised PBS (pH 7.4) containing 5 mM $[Fe(CN)_6]^{-3/-4}$ solution as depicted in **Fig. 5A**. It was observed that the peak current decreased linearly on increasing the concentration of the E2 as analyte (1-100 µM). This is because of the fact that with an increase in concentration, the analyte tends to bind with iron coming from $[Fe(CN)_6]^{-3/-4}$ solution to make an iron complex which retards the analyte to getting onto the electrode surface of the PANI@CeO_2/ITO electrode [[25]. The linear correlation between the peak current and concentration of the analyte is illustrated in **Fig. 5B**, which follows the equation:

$$I = 7.6\times10^{-5}\ A - 9.012\times10^{-8}\ A/\mu M\ [E2];\ R^2 = 0.9865$$

From the slope of the equation, the sensitivity of the biosensor is 142.6 µA μM^{-1} m^{-2}. The fabricated electrode offers LOD of 2.15 µM towards E2 with reference to the equation: LOD= 3σ/S (σ = standard deviation, S = sensitivity obtained from the slope of calibration curve) [[26]. The aromatic ring of E2 consists of hydroxy group which tends to form phenoxyl radical in aqueous medium during the process of oxidation. The radical on further oxidation leads to

formation of corresponding ketone derivative, which conclude the effective electrocatalytic oxidation of E2 using PANI@CeO_2 [27].

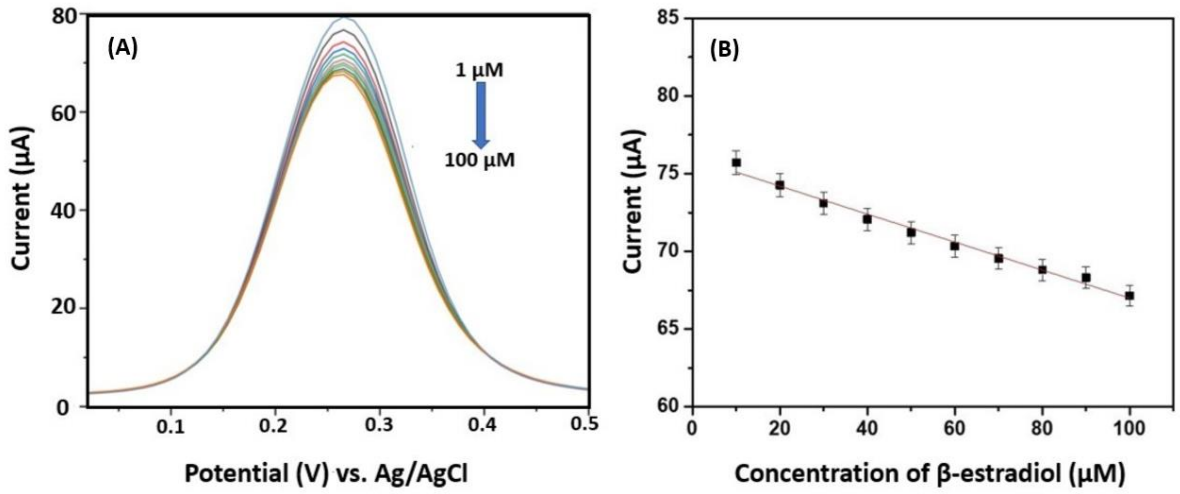

Fig. 5 A) DPV response for PANI@CeO_2 electrode with increase in concentration of beta-E2 as an analyte (1-100 µM); B) Calibration plot between magnitude of current response vs. concentration of the analyte

4.4. Interference, shelf life and stability study

To understand the specificity for analyte E2, an interference study has been performed by testing E2 (100 µM) in presence of equal amount of interferants like ascorbic acid (100 µM), glucose, NaCl, urea, estriol and uric acid which might restrict the sensing of E2 while its detection in urine and water samples. It has been observed from the current response for different interferants, that the target analyte maintained its specificity in different interferants **(Fig. 6A).**

Further, the shelf life of the developed electrode was examined for 21 days in the interval of 7 days. From this study, no change in the current response is observed till 14 days. Whereas a sudden diminution in peak current of around 12.1% is noticed on the 21st day of this study. Thus, we confirm the good stability of the developed biosensor for up to 15 days (**Fig. 6B**).

However, the stability of the biosensing electrode has been confirmed by repeating each result thrice.

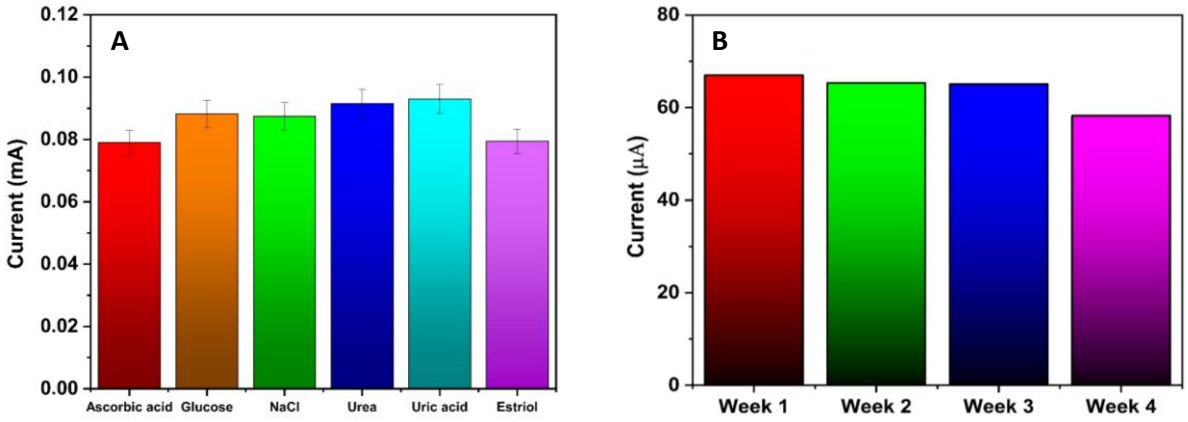

Fig. 6 (A) Interference study for different analytes. (B) Shelf study of the PANI@CeO_2/ITO electrode in 7.4 pH PBS containing 5 mM $[Fe(CN)_6]^{3-/4-}$ for 100 µM E2.

4.5. Real sample analysis

In order to examine the precision and practical applicability of our developed biosensor, we performed electrochemical analysis in two different samples, viz., human urine (Healthy female) and tap water. For analysis, each real sample was infused with different concentrations of E2 (1-100 µM) [28]. From the above analysis, we observed recovery of E2 in the range of 98.3-99.7% for human urine and 97.1-98.1% for tap water which validates the effectuality of the PANI@CeO_2 electrode (Table 2).

TABLE-2

Sample	Added amount (µM)	Found amount (µM)	Recovery (%)
Human urine	10	9.85	98.5
	40	39.88	99.7
	60	59.64	99.4
	100	98.3	98.3

Tap water	10	9.71	97.1
	40	38.92	97.3
	60	58.86	98.1
	100	97.6	97.6

CONCLUSION

In this paper, a novel approach for the detection of E2 has been performed by using non-enzymatic approach. For that, PANI@CeO_2 nanocomposite has been synthesized, characterized and electrophoretically deposited onto ITO. Electrochemical behaviour of PANI@CeO_2 and PANI electrode has been studied. This study depicts that PANI@CeO_2 persist higher current and better diffusion as compared to PANI electrode. A quantitative analysis of three important parameters as sensitivity [275.4 mA $(\mu M)^{-1}$], linear range [1-100 µM] and LOD [2.15 µM] has been obtained. The experiments showed good results which confirm the good repeatability, stability and reproducibility as a non-enzymatic biosensor, which highlights the predominance of our developed biosensor over other non-enzymatic biosensor for the detection of E2. Additionally, a real sample analysis was also verified in human urine and tap water to showcase the applicability of this biosensor.

CRediT authorship contribution statement

Aditya and Tanu: Methodology, data curation, formal analysis, Writing-original draft. S. Verma: Conceptualization, Investigation, & editing. D. Kumar: Supervision, Validation.

Declaration of Competing Interest

The authors declare that they have no known competing financial interests or personal relationships that could have appeared to influence the work reported in this paper.

Data availability

The data that has been used is confidential.

Acknowledgement

Authors thank Dept. of Physics, DTU, Delhi India for XRD facility. S. Verma acknowledges UGC for the JRF Award (NOV 2017-139082).

REFERENCES

[1] J. J. Triviño, M. Gomez, J. Valenzuela, A. Vera, & V. Arancibia, Sensors and Actuators B: Chemical 2019, 297, 126728, https://doi.org/10.1016/j.snb.2019.126728

[2] L. Orozco-Hernández, L. M. Gómez-Oliván, A. Elizalde-Velázquez, R. Natividad, L. Fabian-Castoño, & N. SanJuan-Reyes, Science of The Total Environment 2019, 669, 955-963, https://doi.org/10.1016/j.scitotenv.2019.03.190

[3] A. Nezami, R. Nosrati, B. Golichenari, G. I. RezaeeChatzidakis, A. M. Tsatsakis, & G. Karimi, TrAC Trends in Analytical Chemistry 2017, 94, 95-105, https://doi.org/10.1016/j.trac.2017.07.003

[4] J. Martínez-Guisasola, M. Guerrero, F. Alonso, F. Díaz, J. Cordero & J. Ferrer, Gynecological Endocrinology 2001, 15:1, 14-22, https://doi.org/10.1016/0028-2243(89)90062-2

[5] G. Zhang, T. Li, J. Zhang, & A. Chen, Sensors and Actuators B: Chemical 2018, 273, 1648-1653, https://doi.org/10.1016/j.snb.2018.07.066

[6] M. Nallappan, & M. Gopalan, Materials Research Bulletin 2018, 106, 357-364, https://doi.org/10.1016/j.materresbull.2018.05.025

[7] V. Mooss, Y. Kesari, & A. Athawale, Journal of Materials NanoScience 2022, 9(1), 37-46, https://pubs.thesciencein.org/journal/index.php/jmns/article/view/286

[8] B. Goswami, & D. Mahanta, ACS omega 2021, 6(27), 17239-17246, https://doi.org/10.1021/acsomega.1c00983

[9] S. Paneru, & D. Kumar, Applied Biochemistry and Biotechnology 2023, 1-18, https://doi.org/10.1007/s12010-023-04350-y

[10] X. Huang, N. Hu, R. Gao, Y. Yu, Y. Wang, Z. Yang. & Y. Zhang, Journal of Materials Chemistry 2012, 22(42), 22488-22495, https://doi.org/10.1039/C2JM34340A

[11] C. Liu, H. Tai, P. Zhang, Z. Yuan, X. Du, G. Xie, & Y. Jiang, Sensors and Actuators B: Chemical 2018, 261, 587-597, https://doi.org/10.1016/j.snb.2017.12.022

[12] Y. Shen, Y. H. Lin, & C. W. Nan, Advanced Functional Materials 2007, 17(14), 2405-2410, https://doi.org/10.1002/adfm.200700200

[13] T. Zhou, J. W. Zha, Y. Hou, D., Wang, J. Zhao, & Z. M. Dang, ACS applied materials & interfaces 2011, 3(12), 4557-4560, https://doi.org/10.1021/am201454e

[14] A. A. Ansari, G. Sumana, R. Khan, & B. D. Malhotra, Journal of Nanoscience and Nanotechnology 2009, 9(8), 4679-4685, doi: 10.1166/jnn.2009.1085

[15] M. Beygisangchin, S. Abdul Rashid, S. Shafie, A. R. Sadrolhosseini, & H. N. Lim, Polymers 2021, 13(12), 2003, https://doi.org/10.3390/polym13122003

[16] M. A. Hussein, A., Khan, & K. A. Alamry, RSC advances 2022, 12(49), 31506-31517, https://doi.org/10.1039/D2RA05041B

[17] Y. Lei, Z. Qiu, N. Tan, H. Du, D. Li, J. Liu, T. Liu, W. Zhang, X. Chang, Progress in Organic Coatings 2020, 139, 105430, ISSN 0300-9440, https://doi.org/10.1016/j.porgcoat.2019.105430

[18] N. Parvatikar, S. Jain, S. V. Bhoraskar, & M. V. N. Ambika Prasad, Journal of applied polymer science 2006, 102(6), 5533-5537, https://doi.org/10.1002/app.24636

[19] J. Saranya, S. B.S., P. Gurunathan, R. Sankararajan, M. Thiyagarajan, J Inorg Organomet Polym 2020, 2666–2676, https://doi.org/10.1007/s10904-019-01403-w

[20] H. Huang, & Z. C. Guo, Materials Science Forum 2010, 663–665, 686–689, https://doi.org/10.4028/www.scientific.net/MSF.663-665.686

[21] S. Wang, Z. Huang, J. Wang, Y. Li, & Z. Tan, Journal of Thermal Analysis and Calorimetry 2011, 107(3), 1199–1203, https://doi.org/10.1007/s10973-011-1777-1

[22] N. Elgrishi, K. J. Rountree, B. D. McCarthy, E. S. Rountree, T. T. Eisenhart, J. L. Dempsey, J. Chem. Educ. 2018, 95, 197−206, https://doi.org/10.1021/acs.jchemed.7b00361

[23] E. Laviron, J. Electroanal. Chem. Interfacial Electrochem.101 1979, 19−28, https://doi.org/10.1016/S0022-0728(79)80075-3

[24] O. Jalil, C. M. Pandey, & D. Kumar, Bioelectrochemistry 2021, 138, 107733, https://doi.org/10.1016/j.bioelechem.2020.107733

[25] J. Li, S. Liu, J. Yu, W. Lian, M. Cui, W. Xu, J. Huang, Sensors and Actuators B: Chemical 2013, 188,2013,99-105, ISSN 0925-4005, https://doi.org/10.1016/j.snb.2013.06.082

[26] S. Verma, C. M. Pandey, & D. Kumar, New Journal of Chemistry 2022, 46(44), 21190–21200, https://doi.org/10.1039/D2NJ04285A

[27] J. Li, J. Jiang, D. Zhao, Z. Xu, M. Liu, P. Deng, X. Liu, C. Yang, D. Qian, H. Xie, Journal of Alloys and Compounds 2018,769, 566-575, ISSN 0925-8388, https://doi.org/10.1016/j.jallcom.2018.08.016

[28] P. Supchocksoonthorn, M. C. A. Sinoy, M. D. G. de Luna, P. Paoprasert, Talanta 2021, 235,122782, ISSN 0039-9140, https://doi.org/10.1016/j.talanta.2021.122782